# Collision avoidance for nanosatellite clusters using millimetre-wave radiometric motion sensors

David C. Goodfellow*[a] and Derek Abbott[a]

[a]Centre for Biomedical Engineering (CBME) and
Centre for High Performance Integrated Technologies and Systems (CHiPTec),
Department of Electrical and Electronic Engineering, The University of Adelaide,
SA 5005, Adelaide, Australia.

## ABSTRACT

With the future direction in satellite technology promising to be the production of nanosatellites,[1] very small satellites no heavier than 10 kg or larger than 15 cm, operating in groups or clusters, the ability to detect and avoid collision is not known. Perhaps with the smaller size, the effects of solar, planetary and cosmic radiation[2] in overwhelming the radiometric signal from another satellite is quite large, degrading the chances for collision avoidance.

This paper predicts the sensitivities[3] of our mm-wave collision avoidance sensors[4] for the orbital environment. The effects of strong radiation sources and the dynamics of satellite heating and motions are explored. Methods and techniques for obtaining this information are discussed.

**Keywords:** mm-Wave sensors, Collision avoidance sensors, Radiometry, Nanosatellite clusters, Integrated antenna arrays

## 1. INTRODUCTION

Smaller satellites lead to the need for smaller on-board guidance systems. Indeed the direction for nanosatellites[1,5–7] appears to be for them to function in large clusters. For some applications the cluster can be designed to exhibit "collective behaviour" rather like an insect colony, for the purposes of regrouping and/or adapting the effective communications aperture. Biologically inspired control systems for such clusters are also attracting interest.[8–10] Along with these systems will be the need for sensors for collision avoidance. In accordance for low interference with any communications or telemetric circuitry these sensors should passively detect motion. Radiometric sensors can be employed for this purpose in much the same way as they are used on satellites now for the remote sensing of the Earth's atmosphere and surface.[3,11–14]

By implementing such a sensor in the millimetre-wave band[15] of the electromagnetic spectrum (30 – 300 GHz) a very compact, low weight system can be gained which will integrate well with the small size of a nanosatellite structure. The use of a fully integrated sensor with primary applications in automobile collision avoidance[4,16] is investigated for this possible application. System design and considerations for nanosatellite integration are discussed.

## 2. RADIOMETRIC COLLISION AVOIDANCE

A common radiometer consists of an RF receive antenna array feeding an IF mixing stage which feeds a detection stage. The radiometer essentially takes a measurement of the radiation temperatures of objects in the field-of-view of the array. If the relative temperatures of different objects are compared or if they are compared to the background levels, then these objects can be discerned and characterised. By implementing *insect vision* algorithms[17–19] in the post-processing of the detection stage the relative motions of these objects can be found. This process relies on the ability of the radiometer system to distinguish between the different objects. A direct measure of this ability is the sensitivity of the radiometer. Simply put sensitivity is the smallest temperature difference that is detectable.

*Correspondence: E-mail: dcgoodfe@eleceng.adelaide.edu.au; Telephone: 61 8 8303 3403; Fax: 61 8 8303 4360

Part of the SPIE Conference on Electronics and Structures for MEMS
Royal Pines Resort, Queensland, Australia • October 1999
SPIE Vol. 3891 • 0277-786X/99/$10.00

## 2.1. Sensitivity

A radiometer takes the output power of the antenna over a particular bandwidth $B$ and can amplify this by an amount $G$ before presenting it in a suitable fashion to the detector. For a direct detection radiometer the output is just the power received, given by

$$P = k\,B\,G\,(T_A + T_N), \tag{1}$$

where $k$ is Boltzmann's constant, $G = 1$, and $T_A$ and $T_N$ are the antenna temperature and noise temperature of the system, respectively. The sensitivity relies on the antenna temperature, the noise temperature, the bandwidth and the integration time $\tau$ of the detector in the following way

$$\Delta T = \frac{T_A + T_N}{\sqrt{B\,\tau}}. \tag{2}$$

Skou[3] quotes typical values for these: an antenna temperature of say 200 K; a noise temperature of 800 K; a bandwidth of 100 MHz; and an integration time of 10 ms, which lead to a sensitivity (or standard deviation of output signal) of $\Delta T = 1$ K.

Apart from sensitivity, another important factor is the absolute accuracy of the system. That is, losses in the radiometer feeds can cause a slight change in the measured temperature value. It can be shown that this difference $T_D$ is given by

$$T_D = \ell\,(T_0 - T_1), \tag{3}$$

where $T_0$ and $T_1$ are the physical and input temperatures of the feed, respectively and $\ell$ is the loss of the feed. For a well designed feed system these losses are small, but even for losses as small as 0.01 dB with $T_0 = 300$K and $T_1 = 100$K, the difference, $T_D$ is 0.5 K. This loss corresponds to a reflection coefficient of -26 dB, thus it is important to maintain a reflection coefficient better than this value.[3]

These effects must be considered when designing the feed system. This design is now discussed.

## 2.2. Sensor

The radiometric system under investigation employs a beamforming lens which allows simultaneous scanning through a linear antenna array over a large field of view. The advantages of using this technology is the inherent wide bandwidth of the lens due to a frequency independent structure, the possibility of full integration with detection circuitry at high mm-wave frequencies and the ability to employ insect vision motion detection algorithms through input/output channel discrimination. The front-end system topology for operation at 37 GHz using microstrip integrated circuit technologies at mm-wavelengths (MMIC) was presented in Goodfellow *et. al.*[4] and is briefly described here for higher frequencies.

The linear array for use at a planar single chip level is a 10 element half-wavelength folded dipole antenna array, allowing five beams through a Rotman lens system.[4,20] A schematic of the system is shown in Fig. 1. At 94 GHz the front-end microstrip system has an aperture width of 22 mm and a length of some 35mm, which incorporates the feed lengths. The theoretical radiation pattern of this system is shown in Fig. 2, showing a scan coverage of $\pm 26°$ for beams of 5° beamwidth and sidelobe levels of -16 dB. The losses through the system derive from the microstrip losses into the substrate media through surface wave propagation[21]; the input feed microstrip-to-lens medium transition; lens losses due to spillover and abberations[4,20,22]; the lens-to-microstrip output feeds; and losses in the detection stage on chip (amplification and mixers for downconversion to IF etc). From Section 2.1 the losses that will effect the absolute accuracy of the radiometer are the losses associated with the lens and lens feeds. Through appropriate design these losses can be kept to a minimum at levels of or below 0.01 dB as quoted before.

The importance of the absolute accuracy and sensitivity of the system depends greatly on the signal levels being detected. If the background radiometric temperature levels are close to the temperature levels of the satellite structures strict tolerances in the temperature resolution of the system will have to be applied. The temperatures expected must be investigated to determine these tolerances.

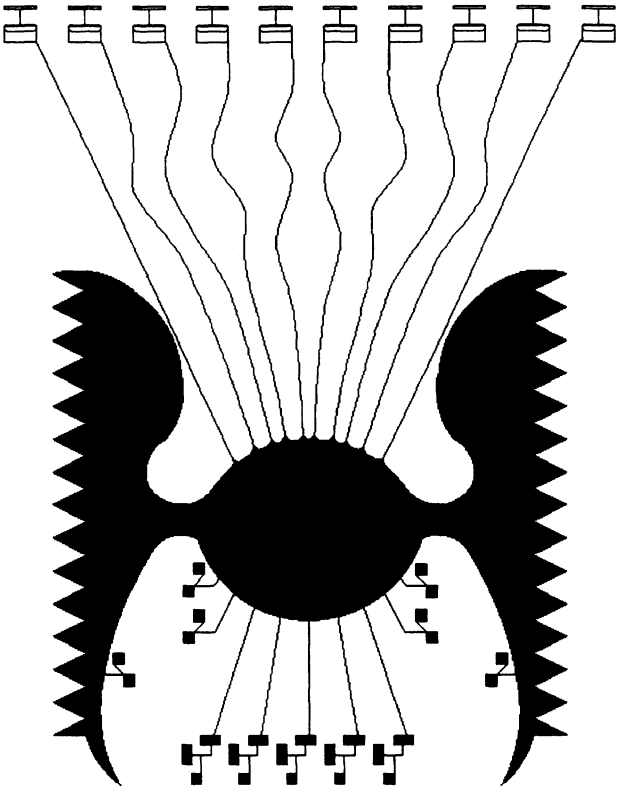

**Figure 1.** Schematic of 5 beam microstrip Rotman lens system showing 10 element folded dipole array with matching circuitry, microstrip feeds to array and beam ports, dummy ports with dissipative loads and output circuitry.

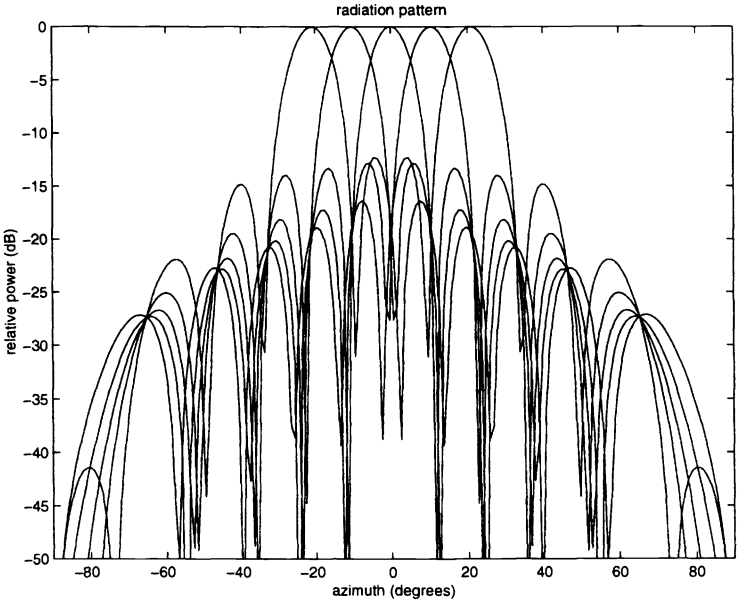


**Figure 2.** Calculated radiation pattern for 5 beam Rotman lens.

At higher frequencies, > 90 GHz, full scale integration is possible. That is, the motion detection system can be completely fabricated onto a single chip if a linear antenna array is used. Several of these sensors can be distributed across the surfaces of a nanosatellite allowing complete coverage of the immediate scene. For radiometric collision avoidance the fundamental consideration is the ability of the sensor to discern the signals of incoming colliding objects from the background. In order to ascertain whether or not a satellite fitted with a radiometric motion sensor could successfully detect another satellite the *brightness temperature* [3] of that satellite needs to be calculated and compared to the brightness temperatures of the Sun, Earth and the cosmic background radiation.

The most convenient method to obtain these values is to consider their blackbody curves or Planck-law distributions. To do this the temperatures of the above need to be known. Firstly, the surface temperature of the Sun is calculated.

## 3.1. The Sun

The surface temperature of the Sun can be calculated since we know the value of the solar energy flux[2] $S$ at the top of the Earth's atmosphere is 1.38 $\mathrm{kWm^{-2}}$. In order to determine the temperature, the total radiated power from the Sun needs to be calculated. This is done by first assuming that the Sun radiates uniformly in all directions, such that it is just the solar radiation flux at the Earth multiplied by the area of a sphere of radius equal to the mean Sun–Earth distance, $1.5 \times 10^{11}$m. Thus,

$$P = S \times 4\pi R^2 \tag{4}$$

$$= 3.90 \times 10^{26} \text{ Watts.}$$

Now if we assume that the Sun is a blackbody radiator, the total power emitted by the Sun is given by

$$P = kAT^4, \tag{5}$$

where $A = 4\pi R_S^2$ is the surface area of the Sun (and $R_S$ is the radius of the Sun, $7 \times 10^8$ m), $k$ is Boltzmann's constant, $5.67 \times 10^{-8}\mathrm{W\,m^{-2}\,K^{-4}}$, and $T$ is the surface temperature. Thus, rearranging Eq.(5) yields the Sun's surface temperature

$$T = \left(\frac{P}{kA}\right)^{1/4}, \tag{6}$$

$$= 5.78 \times 10^3\,\mathrm{K} \approx 5800\,\mathrm{K}.$$

From this we can now calculate the equivalent blackbody temperature of the Earth.

## 3.2. The Earth

By assuming that the Earth is in radiative equilibrium its temperature can be calculated. This is done by firstly calculating the irradiance of planetary radiation $E$ emitted into space by considering the radiative equilibrium condition, incoming flux = outgoing flux

$$(1 - a)S\pi R_E^2 = E4\pi R_E^2, \tag{7}$$

where $a$ is the planetary *albedo** and $R_E$ is the radius of the Earth. Therefore, rearranging Eq.(7) we are left with the following, which yields the Earth's irradiance

$$E = \frac{1}{4}(1 - a)S,$$

$$= 241\,\mathrm{W\,m^{-2}}.$$

We now assume that the Earth is radiating as a blackbody, so we can use the *Stefan–Boltzmann law*

$$E = \sigma T^4, \tag{8}$$

*The planetary albedo is the fraction of the total incident solar radiation that is reflected back into space without absorption. The Earth's albedo is 0.30.

where $\sigma$ is the Stefan–Boltzmann constant, equal to the Boltzmann constant $k$. Therefore, the equivalent blackbody temperature of the Earth is gained by rearranging Eq.(8)

$$T_E = \left(\frac{E}{\sigma}\right)^{1/4},$$

$$= 255\,\mathrm{K},$$

where $T_E$ is known as the effective temperature of the Earth.

### 3.3. The Cosmic Background

Apart from radiating bodies such as the Sun and Earth, there also exists a microwave background radiation.[23,24] That is the universe that is accessible to us on Earth contains radiation approximately like that of a blackbody in the microwave spectrum. This radiation which has a temperature of 2.75 K, is believed to be the remnants of the *big bang*. The existence of this constant background radiation level in the band that we are interested in could have an effect on any radiometric measurements taken and so it is important to consider this radiation.

## 4. BRIGHTNESS CALCULATIONS

The blackbody curve or the Planck's law distribution[25,14] of a body is a useful tool in telling us how that body radiates along the entire electromagnetic spectrum. The distribution measures the *brightness* of the object against either frequency or wavelength. For convenience we chose to look at brightness with wavelength. The brightness of a blackbody radiator in wavelengths is determined by[2]

$$B_\lambda = \frac{2hc^2}{\lambda^5 e^{hc/kT\lambda} - 1}, \tag{9}$$

where $\lambda$ is the wavelength, $h$ is Planck's constant, $6.63 \times 10^{-34}$Js, $c$ is the speed of light, $k$ is again Boltzmann's constant and $T$ is the temperature of interest. The blackbody curves representing the brightness with wavelength values for the Earth, Sun and the cosmic background are shown in Fig. 3, with the mm-wave band shown in bold. Comparison of the brightness values in this region with those of a satellite will provide information about the possibility of detection. Thus, the brightness values for the satellite need to be calculated.

### 4.1. The Satellites

We consider a small perfectly black spherical satellite in orbit around the Earth. Orbit height defines the solid angle subtended by the Earth as seen from the satellite, as in Fig. 4. The axial angle $\psi$ is determined by the right angle triangle involving the radius of the Earth and the distance from the Earth, such that

$$\psi = \mathrm{a\,sin}\,\frac{R_E}{R_E + R}. \tag{10}$$

The solid angle is then calculated using the following equation

$$\Omega = \int_0^{\psi} \sin\phi\, d\phi \int_0^{2\pi} d\theta. \tag{11}$$

Now to calculate the radiative equilibrium temperature of the satellite in the Earth's shadow we consider the amount of heat imparted to the satellite by the Earth, $dQ$. This is given by

$$dQ = \pi r^2 dE = \pi r^2 L d\Omega, \tag{12}$$

where $r$ is the radius of the satellite and $L$ is the radiance of the radiation emitted by the Earth. This can be determined by considering the radiation emitted from an infinite plane surface with uniform radiance in all directions, such that $E = \pi L$. Therefore, Eq.(12) becomes

$$dQ = r^2 E d\Omega. \tag{13}$$

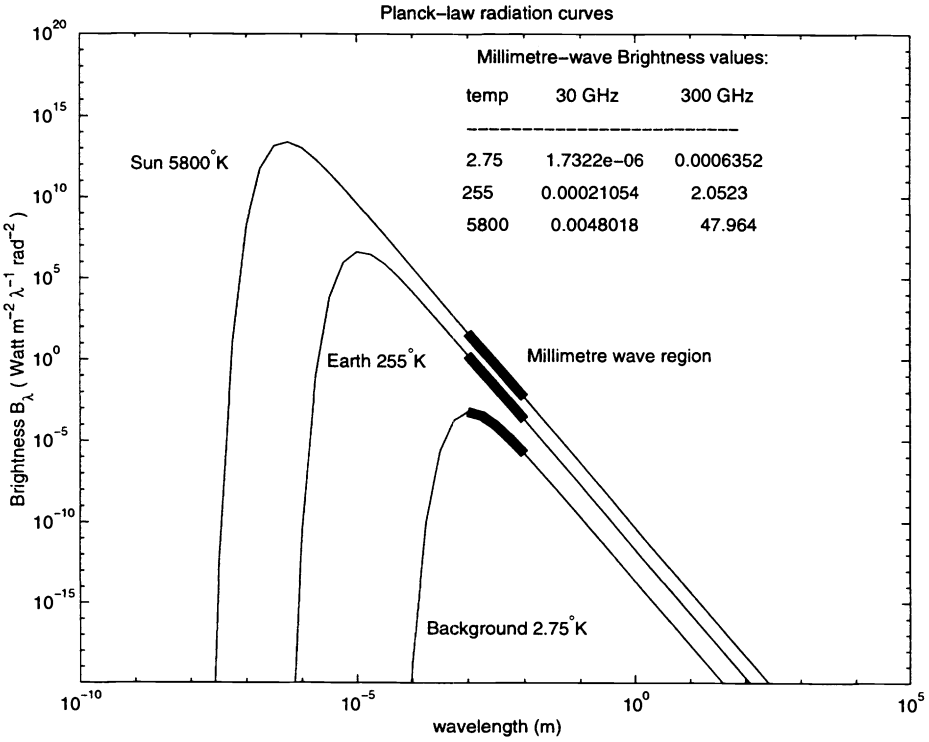


**Figure 3.** Blackbody brightness vs. temperature curves for earth, the sun and the cosmic background.

So if we integrate this over the entire arc of solid angle $\Omega$ we get

$$Q = \Omega r^2 \sigma T_E^4. \tag{14}$$

But, the heat is also given by $Q = AE$, therefore

$$4\pi r^2 \sigma T_S^4 = \Omega r^2 \sigma T_E^4,$$

which becomes

$$T_S = T_E \Big(\frac{\Omega}{4\pi}\Big)^{1/4}. \tag{15}$$

This temperature is modified when the satellite comes out of the Earth's shadow where it is also heated by the Sun. Thus, Eq.(15) becomes

$$T_S^4 = \frac{1}{4}\Big(\frac{R_{sun}}{D}\Big)^2 T_{sun}^4 + \frac{1}{4}\Big(\frac{\Omega}{\pi}\Big) T_E^4, \tag{16}$$

where $D$ is approximately the Earth–Sun mean distance minus the satellites distance from the Earth. From these temperature values the brightness values of the satellite can now be determined. Yet, in order to determine the radiometric signal levels from these brightness values the corresponding *brightness temperatures* need to be calculated.

## 5. BRIGHTNESS TEMPERATURE CALCULATIONS

The brightness temperature is related to the brightness in wavelengths by the following

$$T_B = \frac{\lambda^4 B_\lambda}{2ck\Delta\lambda}. \tag{17}$$

For reasons of simplicity we firstly calculate the brightness temperatures for a single frequency such that the bandwidth $\Delta\lambda$ is unity. The radiometer detects this brightness temperature as an increase in antenna temperature $T_A$, where

$$T_A = \eta T_B, \tag{18}$$

where $\eta$ is the main antenna beam efficiency, which for a good system is of the order of 95%. Thus, the sidelobe beam efficiency of the radiation pattern is $(1-\eta)$, which is 5% in the above case. The contributions of the main and secondary beams on brightness temperature detection are as follows

$$T_A = \eta T_{ml} + (1-\eta)T_{sl}, \tag{19}$$

where $T_{ml}$ and $T_{sl}$ are the main lobe and sidelobe brightness temperatures respectively.

Therefore, if a satellite passes into the main lobe of a radiometer fitted on another satellite, it's brightness temperature will be detected along with possible sidelobe contributions from the Sun, Earth and cosmic background, such that Eq.(19) becomes

$$T_{Asat} = .95T_{Bsat} + .05(T_{Bsun} + T_{Bearth} + T_{Bcb}). \tag{20}$$

Fig. 5 shows the brightness and antenna temperatures calculated for satellites in the Earth's shadow and in full sunlight at various orbit heights from 400 km (LEO) to 2000 km using Eq.(20). As expected the effect of the Earth and background brightness temperatures on the eclipsed satellite antenna temperature is small. The extra contribution from the Sun's brightness temperature almost doubles the antenna temperature, displaying the effect of solar heating.

For a complete analysis it is important therefore to track the satellite temperature through a complete orbit of approximately 92 minutes. This analysis was carried out by Müncheberg *et. al.* for 10 kg aluminium nanosatellites with cubic dimensions of 5, 7.5, 10, 12.5 and 15 cm and heat capacity of 880 $\mathrm{J\,kg^{-1}\,K^{-1}}$ at 400 km orbits, the results shown in Fig. 3 of Müncheberg *et. al.*.[1] The maximum and minimum equilibrium temperatures are equivalent for different sized satellites, since the amount of absorbed and then re-radiated energy is proportional to the surface area of the satellite. Müncheberg *et. al.* showed that the satellite temperature never reached the equilibrium limits through the orbit, rather they ranged between the two. Basically not enough time elapsed in either eclipsed or full sun regions such that the satellite could sufficiently heat or cool.

The range of temperatures fall well inside the temperatures of the Earth, Sun and cosmic background, thus detection of a satellite will be reliable for even low radiometric sensitivities and since absolute measurements of the temperatures are not sought the absolute accuracy is of little relevance. Some cases may not be as straightforward though, such as if a possibly colliding satellite is coming from a direction aligned with the Earth or Sun directions. In this case the main beam of the detector will be washed out at these temperature levels. An absolute temperature measurement would be of greater importance in this situation, since the brightness temperatures of the satellite and radiating body would be superimposed, yielding a larger temperature value being measured than with no satellite present. This temperature rise could be used as a trigger for collision warning.

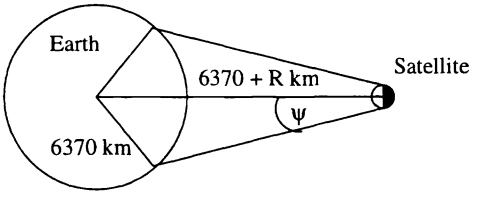


**Figure 4.** Solid angle subtended by Earth on satellite.

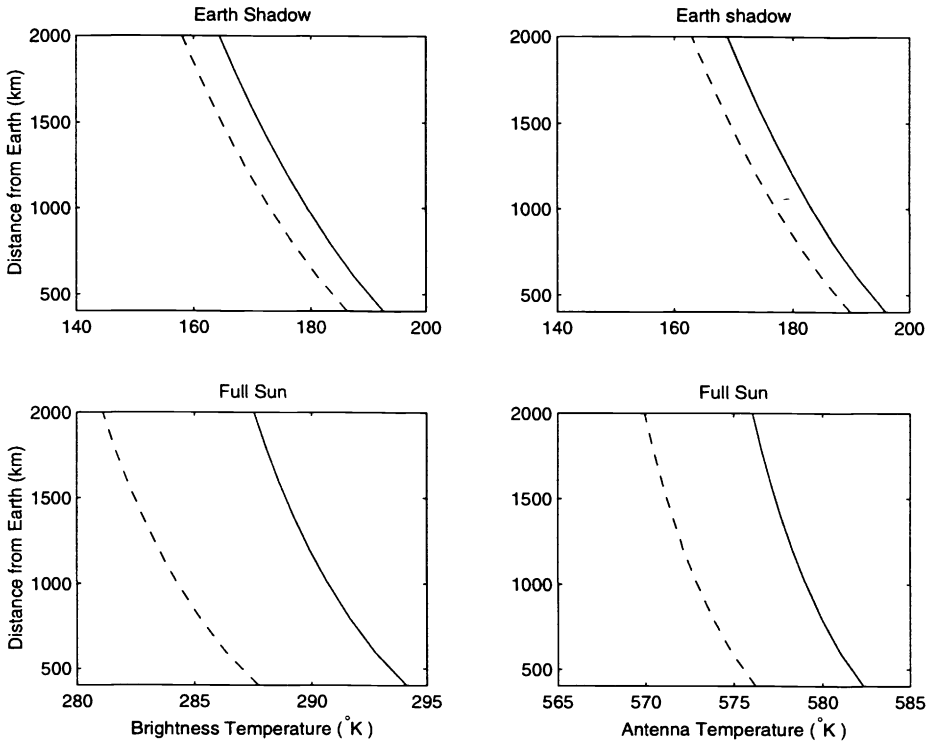


**Figure 5.** Antenna and brightness temperatures for different satellite orbit heights. Solid line shows 300 GHz values, dashed line shows 30 GHz values.

## 6. CONCLUSIONS AND DISCUSSIONS

The radiometric temperatures of nanosatellties in the orbiting environment have been explored. The use of a radiometric collision avoidance sensor to allow safe passage through the orbit for a cluster of nanosatellties has been discussed. The radiometric temperatures of the nanosatellites at various orbit heights lie well below the temperatures of the nearest radiation sources, the Earth and the Sun, and well above the cosmic background level. The scan size and beamwidths of the individual beams from the lens system could be decreased to allow more precise detection of satellites in Earth and Sun paths. Yet this will decrease the ability of detection over a wider field of view. This can be overcome by using more beams, but this will increase the size of the antenna array and therefore the entire system. Many trade-offs exist in the design where losses, size, weight and reliability are important factors.

More intensive investigations can be carried out in the future if this type of technology is indeed required for nanosatellite clusters. Such as the effect of satellite spin, arbitrary shape and use of range measurements for cluster geometries. In conclusion it appears that a fully integrated radiometric motion sensors may be a feasible instrument for collision avoidance for nanosatellites in Earth orbits.

## ACKNOWLEDGMENTS

This work has been kindly funded by the Australian Research Council (ARC), and the Sir Ross & Sir Keith Smith Fund. The antenna front-end design is being designed in collaboration with A. J. Parfitt, CSIRO, NSW.

## REFERENCES

1. S. Müncheberg, M. Krischke, and N. Lemke, "Nanosatellites and microsystems technology – capabilities, limitations and applications," *Acta Astronautica* **39**(9-12), pp. 799–808, 1996.
2. J. M. Wallace and P. V. Hobbs, *Atmospheric Science: an introductory survey*, Academic Press Inc., USA, 1977.
3. N. Skou, *Microwave radiometer Systems: design and analysis*, Artech House Inc., USA, 1989.

4. D. Goodfellow, G. Harmer, and D. Abbott, "mm-wave collision avoidance sensors: future directions," *Proc. SPIE Sensing and Controls with Intelligent Transportation Systems* **3525**, pp. 352–362, (Boston, USA), 1-5 Nov 1998.
5. J. R. Stuart and J. G. Stuart, "Revolutionary next generation satellite communications architectures and systems," *1997 IEEE Aerospace Conference. Proceedings* **3**, pp. 535–545, 1997.
6. A. Hansson, "From microsystems to nanosystems," *J. British Interplanetary Society* **51**, pp. 123–126, 1998.
7. J. R. Stuart, R. R. Coffey, and J. G. Stuart, "Economics of the new smaller and shorter lifetime geostationary communications satellites," *Pacific Telecommunications Council Fifteenth Annual Conference* **2**, pp. 531–536, 1993.
8. J. R. Frigo and M. W. Tilden, "Analog neural network control method proposed for use in a backup satellite control mode," *Proc. SPIE* **3210**, pp. 84–94, 1998.
9. J. R. Frigo and M. W. Tilden, "SATBOT I: prototype of a biomorphic autonomous spacecraft," *Proc. SPIE* **2591**, pp. 66–75, 1995.
10. B. Hasslacher and M. W. Tilden, "Living machines," *Robotics and Autonomous Systems* **15**(1-2), pp. 143–169, 1995.
11. T. J. Jackson and T. J. Schmugge, "Algorithm for the passive remote sensing of soil moisture," in *Microwave Radiomet. Remote Sens. Appl.*, P. Pampaloni, ed., pp. 3–17, 1989.
12. J. C.-C. Shiue and L. R. Dod, "Remote sensing and microwave radiometry," in *Antenna Handbook; theory, applications and design*, Y. T. Lo and S. W. Lee, eds., ch. 22, pp. 1–51, Van Nostrand Reinhold Company Inc., USA, 1988.
13. L. Tsang, J. A. Kong, and R. T. Shin, *Theory of Microwave Remote Sensing*, John Wiley & Sons Inc., USA, 1985.
14. F. T. Ulaby, R. K. Moore, and A. K. Fung, *Microwave Remote Sensing: active and passive, Vol. 1: Microwave remote sensing fundamentals and radiometry*, Addison–Wesley Publishing Company, USA, 1981.
15. K. J. Button and J. C. Wiltse, eds., *Infrared and Millimeter Waves, Vol. 4: Millimeter Systems*, Academic Press Inc., USA, 1981.
16. D. Abbott and A. Parfitt, "Extension of the insect vision paradigm to millimeter waves," *Proc. SPIE* **3207**, pp. 103–106, (Pittsburgh, PA), Oct. 1997.
17. A. Yakovleff, D. Abbott, X. T. Nguyen, and K. Eshraghian, "Obstacle avoidance and motion–induced navigation," *Proc. International Workshop on Computer Architecture for Machine Perception* , pp. 384–393, (Como, Italy), Sept. 1995.
18. G. A. Horridge, "A template theory to relate visual processing to digital circuitry," *Proc. Royal Society of London B* **239**, pp. 17–33, 1990.
19. A. Moini, A. Bouzerdoum, K. Eshraghian, A. Yakovleff, X. T. Nguyen, A. Blanskby, R. Beare, D. Abbott, and R. E. Bogner, "An insect vision-based motion detection chip," *IEEE JSSC* **32**, pp. 279–284, Feb. 1997.
20. W. Rotman and R. F. Turner, "Wide-angle microwave lens for line source applications," *IEEE Trans. Antennas Propagat.* **AP-11**, pp. 623–632, Nov. 1963.
21. D. M. Pozar, "Considerations for millimetre–wavelength printed antennas," *IEEE Trans. Antennas Propagat.* **AP-31**, pp. 740–747, Sept. 1983.
22. M. S. Smith, "Multiple beam crossovers for a lens-fed antenna array," *J. IERE* **55**, pp. 33–36, Jan. 1985.
23. C. Kittel and H. Kroemer, *Thermal Physics, 2nd Edition*, W. H. Freeman and Co., USA, 1980.
24. J. M. Uson and D. T. Wilkinson, "The microwave background radiation," in *Galactic and Extragalactic radio astronomy, 2nd Edition*, G. L. Verschuur and K. I. Kellermann, eds., ch. 14, pp. 606–607, Springer-Verlag New York Inc., USA, 1988.
25. J. Kraus, *Radio Astronomy*, McGraw Hill Inc., USA, 1966.